

# Analysis of additional eddy-current copper losses in large converter-fed hydropower generators

Erlend L. Engevik, Mostafa Valavi and Arne Nysveen

**Abstract**—This paper investigates the effect of converter operation on AC copper losses in the stator and damper windings of a large hydrogenerator. Stator currents are computed using finite element simulations. The computed current waveforms are used as an input to estimate the AC copper losses in the stator due to converter operation using an analytical approach. Damperbar losses are calculated directly in the finite element analysis. The generator is simulated with a two-level voltage source converter and a three-level neutral-point-clamped converter topology. Different carrier frequencies are used to investigate their effect on the AC copper loss. Methods for handling these additional losses are discussed and analysed.

**Index Terms**—converter, copper loss, damperbars, eddy-current, hydrogenerator, pumped-storage hydropower, pulse width modulation

## NOMENCLATURE

$a$	Number of parallel circuits.
$A_{cu,s}$	Stator winding copper cross section (m <sup>2</sup> ).
$b_{c0}$	Width of copper strand (mm).
$b_u$	Width of stator slot (mm).
$D$	Airgap diameter (m).
$f$	Frequency of harmonic (Hz).
$f_{PWM}$	Carrier frequency (Hz).
$f_s$	Synchronous frequency (Hz).
$h_{c0}$	Stator strand thickness (mm).
$I_s$	Stator current (A).
$k_{R,u/l}$	AC resistance factor, upper (u) and lower (l) layer.
$L$	Stator core length (m).
$L_{av}$	Average winding length (m).
$L_\phi$	copper length of one phase winding (m).
$m$	Number of phases.
$P_{cu,dc/ac}$	Stator copper loss, DC and AC (kW).
$Q_s$	Number of stator slots.
$R_{dc/ac}$	DC and AC resistance.
$W_w$	Stator winding coil span.
$z_a$	Number of parallel strands.
$z_t$	Number of strands in one conductor.
$\nu$	Harmonic number.
$\rho$	Conductor resistivity.
$\sigma_c$	Conductor conductivity.
$\xi$	Reduced conductor height.

This work was supported by Norwegian Hydropower Centre (NVKS) and Norwegian Research Centre for Hydropower Technology (HydroCen).

E. L. Engevik (e-mail: erlend.engevik@ntnu.no), M. Valavi and A. Nysveen are with the Department of Electric Power Engineering, Norwegian University of Science and Technology (NTNU), 7034 Trondheim Norway.

## I. INTRODUCTION

Converter operation of large hydrogenerators brings additional current and voltage harmonics that may cause problems with excessive losses and vibration [1]. In copper windings there are both resistive losses due to the DC resistance of the winding cross section and additional AC losses due to skin and proximity effects. When the penetration depth of the winding cross section becomes much larger than the diameter of the strand at the given harmonic frequency, it causes the current to flow along the outer part of the conductor and cause excessive losses.

The eddy current loss in windings increase with the high-frequency harmonics that are produced in converter-operation [2]. Several papers have investigated the effect of converter harmonics on the eddy current losses in stator windings of large induction motors in the MW-range. In [3] the effect of converter-operation on stator winding heating is studied.

It is seen in [4] that the AC copper loss during converter-operation can be in the range from 40 % to 198 % of the DC copper loss. For large hydrogenerators, the heating of the stator is often the limiting factor in the design. For such machines, the AC copper loss can be in the range of 10-15 % of the DC losses. For the generator presented in [5], the AC loss is as high as 30 % of the DC loss.

There are studies presented for converter operation of large synchronous machines in the power range up to 20-30 MVA. Until recently two-level and three-level voltage source converters (VSC) have been used for supplying high-power electrical machines with the largest power ratings. These converters produce rich harmonic spectrums for both voltage and current. Operating generators that are designed for sinusoidal operation with a frequency converter may lead to excessive heating and damages.

No studies have been found that presents the effect of converter operation on the stator winding losses of large hydrogenerators with power ratings above 100 MVA. Grimsel 2 is the largest pumped storage plant with a full-rated converter installed [6] at 100 MW. The Grimsel-converter has a three-level topology with a filter installed in order to use the existing generator without excessive heating. It is therefore not presented any analysis of the additional AC losses in Grimsel 2.

In [7] a modular multilevel converter (MMC) is proposed as the future solution for large converter-fed hydrogenerators. A MMC solution has been shown to drastically reduce amplitude of the harmonic voltages and currents produced by the converter. This allows for using traditional generator designs

without filters. It is shown in [8] that the additional copper losses are relatively high when a two-level topology is used. For a multilevel-topology these losses become negligible.

Many publications have been presented on modeling and prediction of currents and losses in damper windings of large hydrogenerators. It is common practice to use fractional slot windings in large hydrogenerators. These windings produce subharmonics that interact with the damper winding to increase the damperbar losses during normal operation compared to integer slot windings [9].

In [10] an analytical method for calculating damperbar currents and losses are presented. The magnetic field in the airgap is predicted using permeance model that is used as input for an equivalent circuit model. [11] uses permeance data from stationary finite element simulations together with a rotating field model to predict damperbar losses. Both methods are compared to finite element simulations.

A permeance model is used in [12] to compute the induced damperbar voltages using numerical integration. Results are compared to finite element simulations using an external circuit to represent the damper winding. The main reason for this is that damperbar currents are normally not measured during commissioning of electrical machines [13]. There are only a few publications comparing simulations to measurements.

[14] modeled the damper winding in a 2D finite element simulations with acoupled external circuit model. Results are compared indirectly in [15] by temperature measurements on the damperbars and a thermal model where the simulated damperbar losses are used as input. Recently, results from direct measurements of damperbar currents in a large hydro-generator was presented in [16]. The results from [16] was analysed and compared to simulations in [17].

The same voltage and current harmonics that are produced by converter operation induce additional losses in damperbars. A large synchronous motor with salient poles have been analyzed with sinusoidal and converter-fed operation in [18]. It was found that damperbar losses can increase dramatically with converter operation. For converters in the MW-range it is normal to use a low carrier frequency, e.g. 250-450 Hz [19]. It is shown in [19] that additional losses due to converter-operation in this machine is greatly reduced when a three-level topology is used instead of a two-level topology. When a multilevel converter is used, the additional losses become very small.

This paper investigates the effect of converter topology and carrier frequency on the copper losses in a 180-slot/14-pole 105 MVA-generator. Generator and converter specifications are given in Table I. The damper windings are excluded for most of the simulations. Two converter topologies are modeled, first a two-level VSC and then a three-level neutral-point-clamped (NPC) topology. Four carrier frequencies are simulated. First a typical 450 Hz case is simulated. Then 1050 Hz, 2100 Hz and 10500 Hz is used to investigate the effect of possible developments in semiconductor devices.

TABLE I:  
Design specifications

Generator	Power	105 MVA
	Speed	428.6 rpm
	Number of poles	14
	Number of slots	180
	Airgap diameter	3.672 m
	Machine length	1.8 m
Converter	Configuration	2-level, 3-level NPC
	Switches	Ideal
	PWM	Sinusoidal
	Carrier frequency	450 Hz, 1050 Hz 2100 Hz, 10500 Hz

## II. ELECTROMAGNETIC MODELING OF AC COPPER LOSSES

Finite element analysis of the 105 MVA, 180-slot/14-pole generator is used in order to investigate the AC copper losses produced by converter operation. The generator is modeled in 2D using the power electronic circuit that was developed for [1] to investigate possible vibration problems during converter operation.

The power electronic circuit is illustrated in Fig. 1. In order to include the effect of converter switching, a sufficiently small time step was used (i.e 10 microseconds). The converters are modeled with ideal switches and sinusoidal pulse width modulation due to computational considerations.

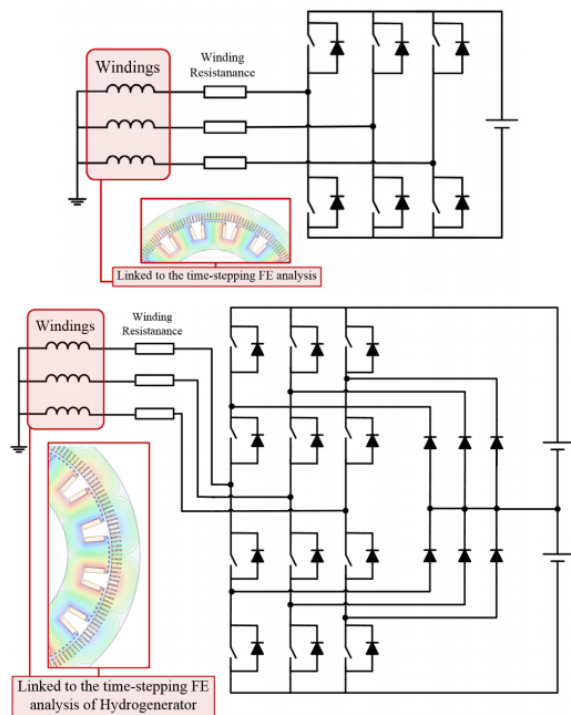


Fig. 1: Coupled converter circuit models used in finite element simulations. two-level VSC (top) and three-level NPC topologies, illustration from [1].

The copper losses in the stator winding of the machine are given by (1), where  $I_s$  is the stator current and  $R_{dc}$  is the DC resistance. The DC resistance is given by (2) where  $\rho$  is the copper resistivity,  $A_{cu,s}$  the stator winding copper cross section, and  $a$  the number of parallel circuits.

$$P_{cu,dc} = 3R_{dc} \cdot I_s^2 \quad (1)$$

$$R_{dc} = \frac{\rho L_\phi}{A_{cu,s} a} \quad (2)$$

The copper length of one phase winding is calculated using (3). Here  $L_{av}$  is the average length of each winding given by (4) [20],  $D$  is the airgap diameter,  $Q_s$  is the number of stator slots and  $W_w$  is the coil span in number of slots.

$$L_\phi = \frac{L_{av} Q_s}{3a} \quad (3)$$

$$L_{av} = 2L + 2.8 \frac{\pi D}{Q_s} W_w + 0.4 \quad (4)$$

In addition to the equivalent DC losses, different harmonic components of the current gives additional copper losses. The current waveform is extracted from the finite element simulation, and a Fourier transform is used to obtain the harmonic spectrum. It is subsequently used as an input for calculating the AC copper loss with (5). After the harmonic spectrum of the stator current is known, the AC resistance is calculated for each harmonic frequency and the AC losses are found using (5) where  $\nu$  denotes the harmonic.

$$P_{cu,ac} = 3 \sum (R_{ac,\nu} - R_{dc}) I_{s,\nu}^2 \quad (5)$$

Each current harmonic experiences its own effective resistance  $R_{ac}$  given by (6), which consist of the AC resistance of the end winding  $R_{end}$  and the AC resistance components from upper layer bar  $R_{ac,u}$  and the lower layer bar  $R_{ac,l}$ . The AC resistance of the end winding is usually considered equal to the DC resistance.

$$\begin{aligned} R_{ac} &= R_{end} + R_{ac,u} + R_{ac,l} \\ &= \frac{R_{dc}}{L_\phi} \left[ \left[ L_\phi - \frac{2LQ_s}{3a} \right] + (k_{R,u} + k_{R,l}) \frac{LQ_s}{3a} \right] \end{aligned} \quad (6)$$

Due to skin and proximity effects, the AC resistance  $R_{ac}$  is  $k_R$  times higher than the DC resistance. In the case of a two-layer winding, the AC resistance factor  $k_R$  is not the same for each layer. The expression for the upper layer  $k_{R,u}$  is given by (7) from [20], while the lower layer resistance factor  $k_{R,l}$  can be calculated by (8).

$$k_{R,u} = \varphi + \frac{z_t^2 - 1}{3} \psi \quad (7)$$

$$k_{R,l} = k_{R,u} \left( 1 + \frac{2z_t^2}{3} \xi^4 \right) \quad (8)$$

Skin effect makes the subconductor height,  $\xi$ , seen by each harmonic given by (9) smaller than the physical strand

thickness  $h_{c0}$  [20].  $z_t$  is the number of strands in the conductor,  $f$  is the harmonic frequency,  $\sigma_c$  is the conductivity of the conductor,  $z_a$  the number of parallel strands,  $b_{c0}$  is the strand width and  $b_u$  the slot width.  $\varphi$  and  $\psi$  given by (10) and (11) are factors that are dependent on the reduced conductor height  $\xi$  [20].

$$\xi = h_{c0} \sqrt{\pi f \mu_0 \sigma_c \frac{z_a b_{c0}}{b_u}} \quad (9)$$

$$\varphi(\xi) = \xi \frac{\sinh 2\xi + \sin 2\xi}{\cosh 2\xi - \cos 2\xi} \quad (10)$$

$$\psi(\xi) = 2\xi \frac{\sinh \xi - \sin \xi}{\cosh \xi + \cos \xi} \quad (11)$$

### III. RESULTS AND DISCUSSION

AC copper losses due to converter operation have been calculated using a combination of finite element simulation and analytical expressions. In Fig. 2 the harmonic spectrum of the stator current is presented for a two-level voltage source converter and a three-level NPC topology using 450 Hz and 1050 Hz as carrier frequency. Current waveforms are shown in Fig. 3.

As discussed in [1], the dominant additional harmonics produced by the converter switching are  $f_{PWM} \pm 2f_s$ ,  $f_{PWM} \pm 4f_s$  and  $2f_{PWM} \pm f_s$ .  $f_{PWM}$  is the carrier frequency and  $f_s$  is the synchronous grid frequency. For the case with a 450 Hz carrier frequency, the dominant harmonic frequencies are then 250 Hz, 350 Hz, 550 Hz, 650 Hz, 850 Hz and 950 Hz. If a 1050 Hz carrier frequency is used, the dominating current harmonic components are found at 850 Hz, 950 Hz, 1150 Hz, 1250 Hz, 2050 Hz and 2150 Hz. Converter switching produce, in addition, even higher frequency current harmonics whose amplitude decrease with increased frequency.

Fig. 2 also shows that the amplitude of the current harmonics are drastically reduced when the two-level converter is replaced with a three-level NPC-topology. With a 450 Hz carrier frequency the total harmonic distortion (THD) is reduced from 5.39 % to 2.47 % by replacing the two-level VSC with a three-level NPC.

It is seen by studying Fig. 2 that the amplitude of the dominant current harmonics is reduced when the carrier frequency is increased from 450 Hz to 1050 Hz. This gives a lower THD than using the 450 Hz carrier frequency. For the two-level topology the THD is 2.66 % and for the NPC the THD is 1.09 %.

Using a higher carrier frequency increase the frequency of the dominating current harmonics produced by converter operation. An increased carrier frequency increase the amplitude of these current harmonics. The net effect of these two mechanisms is that the AC copper losses increase with higher carrier frequencies.

It is observed in Fig. 2 that the presence of damperbars in the rotor will increase the amplitude of the current harmonic components. This results in a much higher THD, 2.25 %,

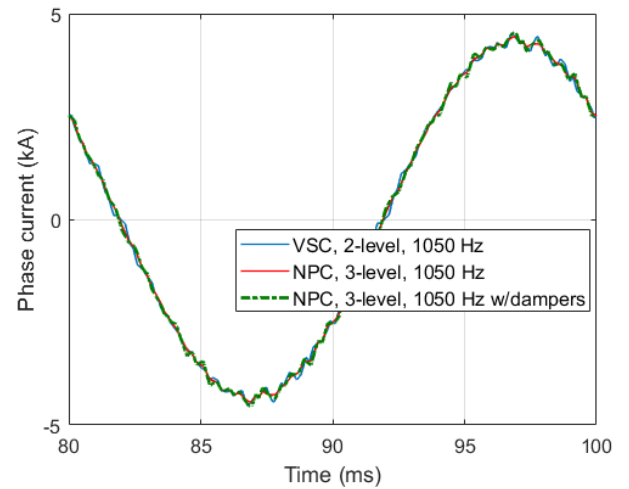
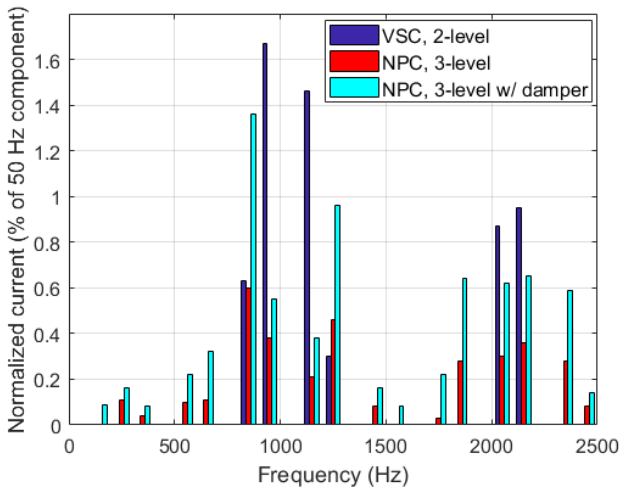
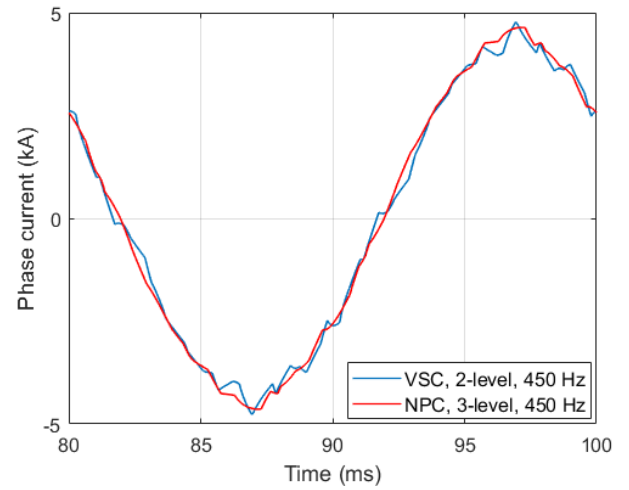
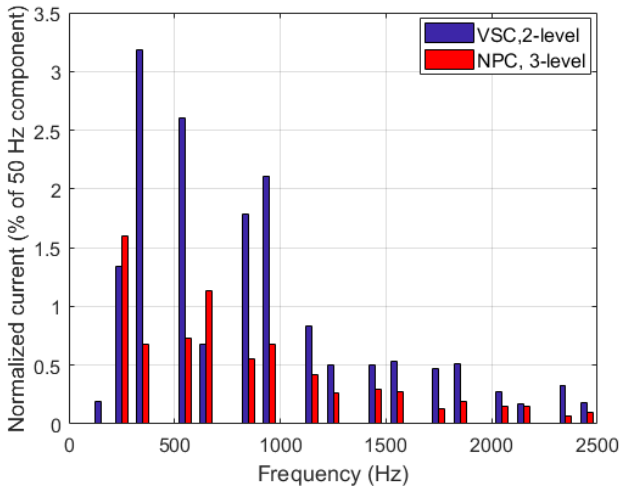


Fig. 2: Time harmonic spectrum of converter-fed stator current at 450 Hz carrier frequency (top), and 1050 Hz carrier frequency.

Fig. 3: Simulated stator current waveforms at 450 Hz carrier frequency (top) and 1050 Hz carrier frequency.

which is twice the THD experienced without damperbars. Part of the reason for this is that having damper bars reduce the total generator inductance experienced by the converter. Having a lower inductance means that the filtering ability of the circuit is lower, which gives higher current amplitudes.

AC copper losses are compared to the AC copper loss for sinusoidal operation in Fig. 4 for the two different converter topologies using 450 Hz and 1050 Hz as the carrier frequency. As can be seen, current harmonics produced by switching increase the AC copper loss from a modest 27.5 kW to between 79 and 485 kW which would cause intolerable heating and probably destroy the winding.

One solution for reducing the AC copper loss is to reduce the strand thickness. The original strand thickness of this generator is 1.8 mm. In order for the DC copper loss to stay constant, the number of strands was increased to keep the total conductor area constant.

The effect of reducing the strand thickness on the AC

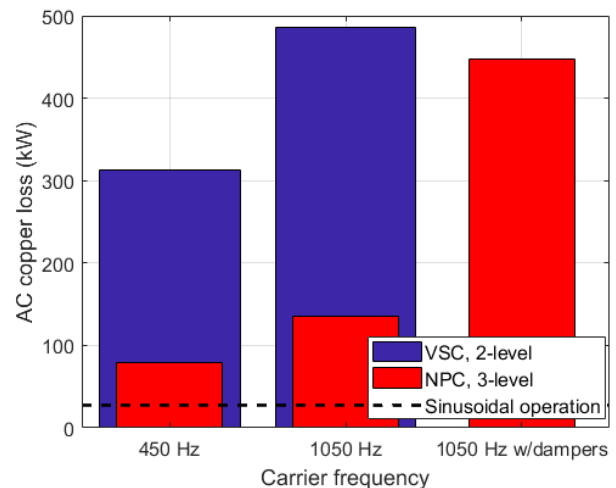


Fig. 4: AC stator copper losses at different carrier frequencies.

copper loss are presented in Fig. 5. One can see that it is possible to achieve the same level of AC losses using the NPC-topology as during sinusoidal operation. Using the lower carrier frequency, i.e. 450 Hz, allow us to reach the original AC copper loss value at a strand thickness of 1.0-1.3 mm. If 1050 Hz is used as the carrier frequency, the strand thickness would have to be reduced to 1.1 mm or below.

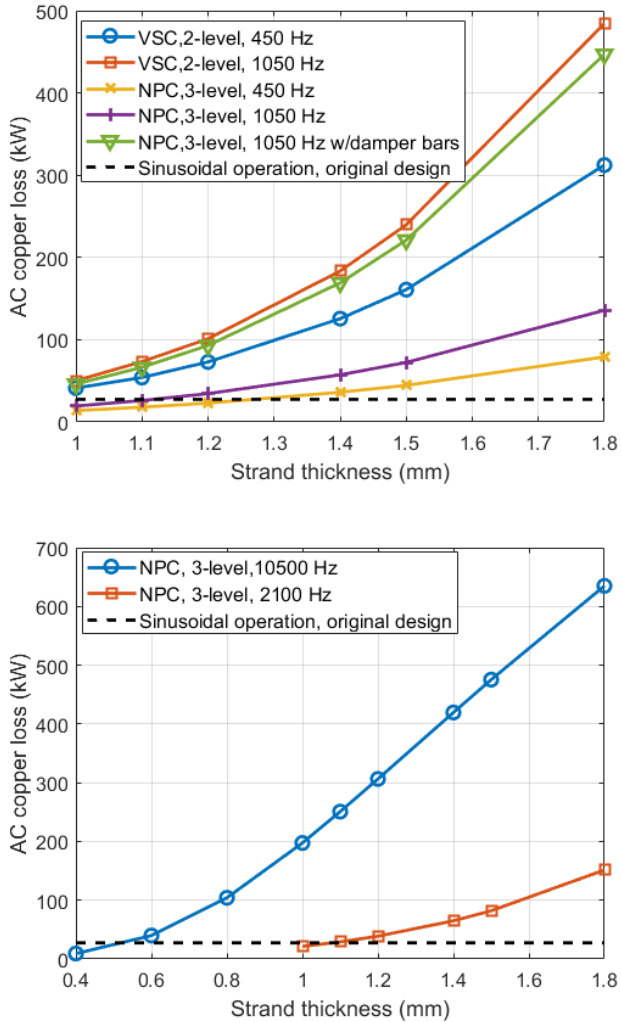


Fig. 5: Comparison of AC copper losses with different converter topologies and winding designs. Carrier frequency of 450 and 1050 Hz (top), and 2100 and 10500 Hz.

Possible developments in semiconductor technology may allow for the use of higher carrier frequencies. In order to investigate this, the generator is simulated with a carrier frequency of 2100 Hz and 10500 Hz. The current harmonic spectrum for the two cases are presented in Fig. 6. It is seen that the amplitude of the current harmonics is reduced when the carrier frequency is increased. The frequency of each harmonic is also higher for higher carrier frequencies.

The net effect on the losses of increasing the carrier frequency to 2100 Hz and 10500 Hz is presented in Fig. 5. It is seen that although the amplitude of the harmonic

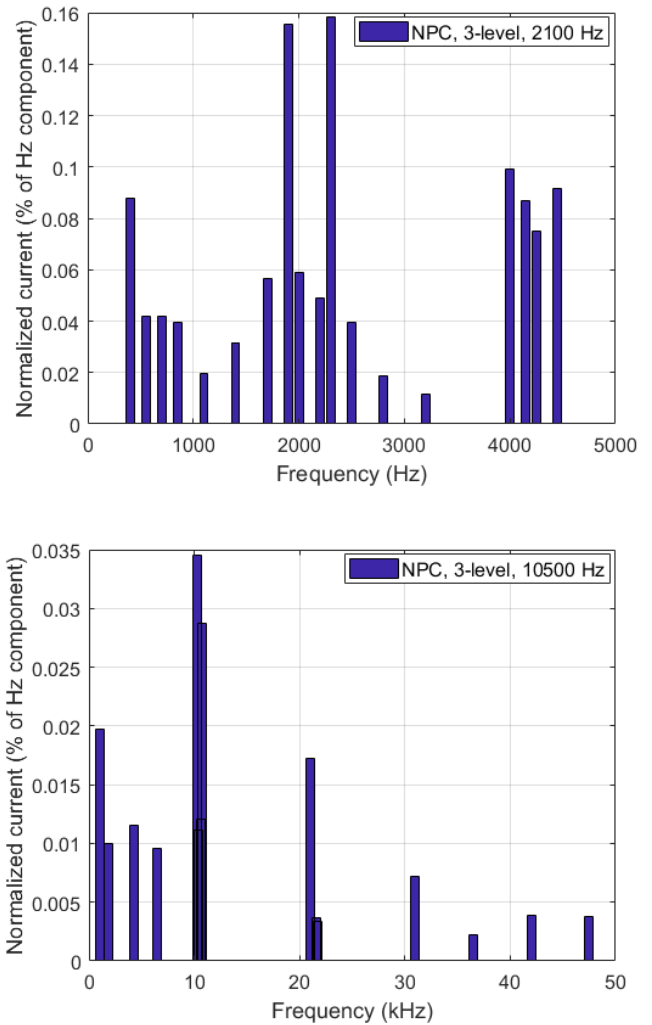


Fig. 6: Time harmonic spectrum of converter-fed stator current at 2100 Hz carrier frequency (top) and 10500 Hz carrier frequency.

currents produced by the converter is small, the AC copper loss increase with increasing carrier frequency. The strand thickness would also have to be reduced to a larger extent for carrier frequencies of 2100 and 10500 Hz than what was the case for 450 and 1050 Hz.

Int the previous paragraph, it was seen that the damper-bars increase the AC copper loss in the stator winding substantially. Converter operation also increase the losses in the damperbars themselves. The two-level VSC topology produces a richer current harmonic spectrum than the three-level NPC topology. This leads to more additional losses with a two-level topology than a three-level topology produce. While the net effect of increasing the carrier frequency on the stator AC copper losses was that the losses increased, the opposite is true for the losses in the damperbars.

Damperbar losses are calculated directly in the finite element software. The additional losses using carrier frequencies of 450 Hz, 1050 Hz and 2100 Hz are listed in Table

II. The resulting losses are 51.9 times, 12.8 times and 5.6 times the losses during sinusoidal operation. The reduction in damperbar losses with increasing carrier frequency is substantial. Thus, using a two-level converter still yields multiple times the damperbar losses experienced in 50 Hz sinusoidal operation, and can therefore not be a viable solution.

It is presented in Table II that the effect of increasing the carrier frequency from 450 Hz to 1050 Hz for the NPC topology is that the losses is decreased from 9.2 times the losses under sinusoidal operation to 3.9 times the losses under sinusoidal operation. By increasing the carrier frequency to 2100 Hz, the damperbar losses are further reduced to 2.3 times the loss under sinusoidal operation. Using a three-level topology is therefore more suitable than the option with a two-level converter, but the increased losses still might cause local heating issues.

There are ways to limit the additional losses in damperbars during converter operation. For the stator winding, reducing the strand thickness reduce the additional AC copper losses caused by converter harmonics. It is possible to utilise this method for the damperbars in a similar way. In Fig. 7, the original damperbar configuration is shown to the left and an alternative damperbar configuration to the right. The total cross section of the damper winding was first kept the same. The difference is that the number of damperbars per pole is increased from 7 to 15, reducing the radius of each damper 68.6 % of its original value. One can see that the radius of the damperbars is too large to reduce the induced damperbar losses, see Alternative configuration I in Table II. Thus, as a result, the losses are increased by one third.

TABLE II:

Damper winding losses in converter operation at unity power factor

Topology/ $f_{PWM}$	Damper bar losses (kW)		
	450 Hz	1050 Hz	2100 Hz
2-level VSC	498.2	123.3	54.1
3-level NPC	88.7	37	22.2
Alternative configuration w/NPC I		49.5	
Alternative configuration w/NPC II		24.6	
Sinusoidal operation	9.6		

By reducing the radius of each damperbar further, the damperbar losses are reduced.. From Table II it is seen that the damperbar losses with alternative damper winding configuration II are reduced by 33.5 % compared to the damperbar loss with the original damperbar configuration. The radius of each bar is set to 46.7 % of its original value. The damperbar loss is still 2.6 times larger than during sinusoidal operation. This shows that the increase in damperbar losses can be reduced by using an alternative configuration for the damper winding. Further optimization of the damper winding configuration might give even better results. It should be noted here that the damping performance of any new configuration has to be checked before any decision or change is made in order to ensure satisfying operation of the generator.

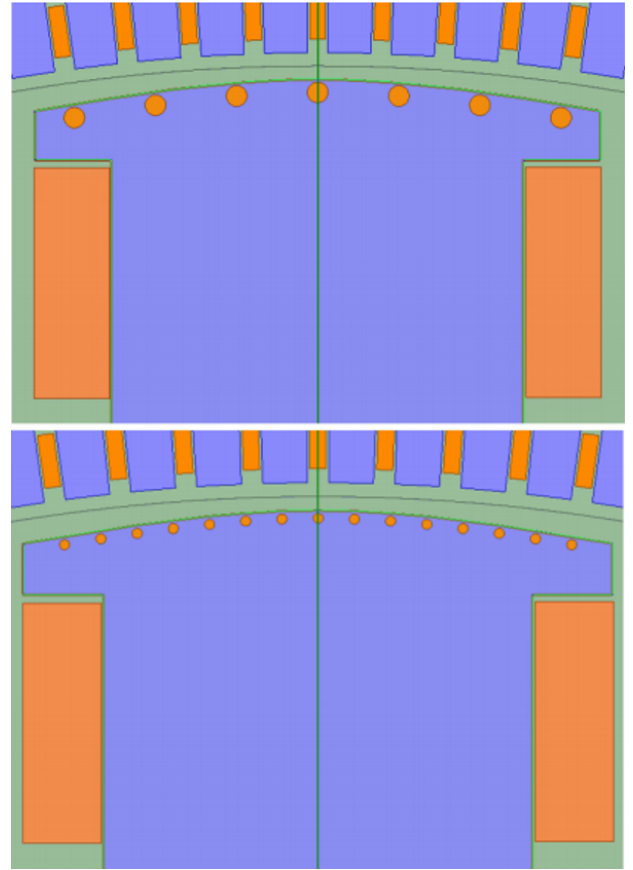


Fig. 7: Alternative damperbar configurations. Traditional 7 bars per pole configuration (top) and alternative 15 bars per pole configuration.

If a generator is built for converter operation using a two-level or a three-level topology like the ones that are industry standard, the strand thickness would have to be reduced compared to traditional designs. Another option is to use a filter between the converter and the generator. This would eliminate the problem with current harmonics. If a frequency converter is to be installed in an existing installation, using a filter will be necessary to avoid excessive heating and damage to the windings.

Based on Fig. 5 and Table II, it is advised against using damperbars when two- or three-level converter topologies are used. Including damperbars in a converter-fed synchronous hydrogenerator without a harmonic filter seems to increase the AC copper losses in the stator. In addition to this, the losses in the damperbars themselves increase with 130 % to 5087.5 % during converter operation. If the generator is to be able to operate directly connected to the grid without the converter, then the damper bars must be included to ensure stable operation. Using a filter between the converter and the generator might then be the only option if a two-level or three-level converter is to be used.

#### IV. CONCLUSIONS

The effect of converter operation on AC copper losses in large hydrogenerators has been investigated. Using a higher carrier frequency increase the frequency of the dominating current harmonics produced by converter operation. An increased carrier frequency decrease the amplitude of these current harmonics leading to a lower total harmonic distortion of the stator current. The net effect of these two mechanisms is, sadly, that the AC copper losses increase with higher carrier frequencies.

Current harmonics produced by switching in two- and three-level converters increase the AC copper losses in traditionally designed stator windings in large hydrogenerators. These additional losses could cause intolerable heating and probably destroy the windings. Using a three-level converter topology instead of a two-level topology gives significant reductions in the AC copper losses.

It is possible to reduce the AC copper losses by reducing the strand thickness in the stator winding. If a generator is going to be built for converter operation using a two-level or a three-level topology like the ones that are available today, the strand thickness would have to be reduced compared to traditional designs. Another option is to use a filter between the converter and the generator.

Including damper bars in a converter-fed synchronous hydrogenerator seems to increase the AC copper losses in the stator. In addition to this, the losses in the damperbars themselves increase substantially. The additional damperbar losses are smaller using a three-level topology than when a two-level topology is used. Increasing the carrier frequency reduces the additional damperbar losses. It seems that changing the damper winding configuration can reduce the additional damperbar losses as well. It is advised against using damper bars if possible when two- or three-level converter topologies are used.

#### REFERENCES

- [1] M. Valavi, E. Devillers, J. Le Besnerais, A. Nysveen, and R. Nilsen, "Influence of Converter Topology and Carrier Frequency on Airgap Field Harmonics, Magnetic Forces, and Vibrations in Converter-Fed Hydropower Generator," *IEEE Transactions on Industry Applications*, vol. 9994, no. c, pp. 1–1, 2018.
- [2] S. Iwasaki, R. P. Deodhar, Y. Liu, A. Pride, Z. Q. Zhu, and J. J. Bremner, "Influence of PWM on the proximity loss in permanent-magnet brushless AC machines," *IEEE Transactions on Industry Applications*, vol. 45, no. 4, pp. 1359–1367, 2009.
- [3] M. J. Islam, H. V. Khang, A. K. Repo, and A. Arkkio, "Eddy-current loss and temperature rise in the form-wound stator winding of an inverter-fed cage induction motor," *IEEE Transactions on Magnetics*, vol. 46, no. 8, pp. 3413–3416, 2010.
- [4] M. J. Islam and A. Arkkio, "Effects of pulse-width-modulated supply voltage on eddy currents in the form-wound stator winding of a cage induction motor," *IET Electric Power Applications*, vol. 3, no. 1, pp. 50 – 58, 2009.
- [5] A. B. M. Aguiar, A. Merkhof, C. Hudon, and K. Al-Haddad, "Influence of the Variation of the Input Parameters on the Simulation Results of a Large Hydrogenerator," *IEEE Transactions on Industry Applications*, vol. 50, no. 1, pp. 261–268, 2014.
- [6] H. Schlunegger and A. Thöni, "100 MW full-size converter in the Grimsel 2 pumped-storage plant," in *Hydro 2013 conference*, Innsbruck, 2013.

- [7] P. K. Steimer, O. Senturk, S. Aubert, and S. Linder, "Converter-fed synchronous machine for pumped hydro storage plants," in *Energy Conversion Congress and Exposition (ECCE), 2014 IEEE*, 2014, pp. 4561–4567.
- [8] O. Drubel, *Converter applications and their influence on large electrical machines*. Springer-Verlag, 2013, vol. 232.
- [9] T. Pham, S. Salon, W. Akaiishi, and M. Debortoli, "Damper bar heating in hydro generators with fractional slot windings," *2017 IEEE International Electric Machines and Drives Conference, IEMDC 2017*, 2017.
- [10] Y. Lu, J. Liu, L. Zhou, and H. Kang, "Analytical calculation of damper winding losses in large hydrogenerators," in *Electrical Machines and Systems (ICEMS), 2014 17th International Conference on*, 2014, pp. 373–377.
- [11] M. Ranlöf and U. Lundin, "The rotating field method applied to damper loss calculation in large hydrogenerators," in *Electrical Machines (ICEM), 2010 XIX International Conference on*, 2010, pp. 1–6.
- [12] G. Traxler-Samek, T. Lugand, and A. Schwery, "Additional Losses in the Damper Winding of Large Hydrogenerators at Open-Circuit and Load Conditions," *Industrial Electronics, IEEE Transactions on*, vol. 57, no. 1, pp. 154–160, 2010.
- [13] *IEC 60034-2-1 Rotating electrical machines - Part 2-1: Standard methods for determining losses and efficiency from tests (excluding machines for traction vehicles)*.
- [14] A. B. M. Aguiar, A. Merkhof, K. Al-Haddad, and C. Hudon, "Electromagnetic modelling of existing large hydro generator," in *Electric Machines & Drives Conference (IEMDC), 2011 IEEE International*, 2011, pp. 389–393.
- [15] A. B. M. Aguiar, "Electromagnetic modeling of large hydro generators using 2D finite element method," Ph.D. dissertation, École de Technologie Supérieure, Université Du Québec, 2014.
- [16] M. Bergeron, J. Cros, J. Niehenke, J. R. Figueroa, and C. Messier, "Hydro generator damper bar current measurement at Wanapum Dam," *IEEE Transactions on Energy Conversion*, vol. 31, no. 4, pp. 1510–1520, 2016.
- [17] A. Z. Gbégbé, B. Rouached, J. Cros, M. Bergeron, and P. Viarouge, "Damper Currents Simulation of Large Hydro-Generator Using the Combination of FEM and Coupled Circuits Models," *IEEE Transactions on Energy Conversion*, vol. 32, no. 4, pp. 1273–1283, 2017.
- [18] P. Rasilo, A. Belahcen, and A. Arkkio, "Effect of Rotor Pole-Shoe Construction on Losses of Inverter-Fed Synchronous Motors," *IEEE Transactions on Industry Applications*, vol. 50, no. 1, pp. 208–217, 2014.
- [19] P. Rasilo, A. Salem, A. Abdallah, F. De Belie, L. Dupré, and J. A. Melkebeek, "Effect of Multilevel Inverter Supply on Core Losses in Magnetic Materials and Electrical Machines," *IEEE Transactions on Energy Conversion*, vol. 30, no. 2, pp. 736–744, 2015.
- [20] J. Pyrhönen, T. Jokinen, and V. Hrabovcová, *Design of Rotating Electrical Machines*, 2nd ed. John Wiley & Sons, Ltd, 2014.

#### V. BIOGRAPHIES

**Erlend L. Engevik (M'15)** was born in Stord, Norway in 1990. He received the M.Sc. degree in energy and environmental engineering from Norwegian University of Science and Technology (NTNU), Trondheim, Norway, in 2014. Currently, he is pursuing a PhD degree from the Department of Electric Power Engineering at NTNU. His main research interest is in design and analysis of electrical machines.

**Mostafa Valavi (S'07 - M'15)** received his PhD degree in 2015 from the Norwegian University of Science and Technology (NTNU), Trondheim, Norway. Since then, he has been a postdoctoral research fellow at NTNU. His research interests include design and analysis of electrical machines.

**Arne Nysveen (M'98 - SM'06)** received his Dr.ing. in 1994 from Norwegian Institute of Technology (NTH). From 1995 to 2002 Nysveen worked as a research scientist at ABB Corporate Research in Oslo, Norway. Since 2002 Nysveen has been a professor at the Norwegian University of Science and Technology (NTNU). He is the Work Package Manager for turbine and generator technologies in Norwegian Research Centre for Hydropower Technology (HydroCen).